momentarily speed up (to a period = $T^* - d + \varepsilon$, where d is a constant increment, and ε is a continuously distributed stochastic variable with mean = 0), but this is necessarily followed by compensatory slowing (to $T^* + d + \varepsilon$). If leading chirps are more attractive and the values of individual chirps are averaged across successive chirp periods to produce an overall index of a male's attractiveness to females, R is an ESS.

None of the hypotheses proposing adaptive, cooperative functions for synchrony in *N. spiza* are tenable. Females did not show an increased latency when orienting to alternated chirps in the arena trials (t-tests for paired comparisons; $P > 0.20$), implying that synchrony did not result from a need to maintain a specific signalling rhythm within a neighbourhood. Unlike certain acoustic orthopterans[20–23], *N. spiza* has no known phonotactic natural enemies, and when we deployed loudspeakers broadcasting male calls in the field for several hours nightly during various seasons neither potential predators nor parasitoids were attracted. It is therefore doubtful that synchrony currently represents a strategy for evading natural enemies. Males are not distributed spatially in dense clusters which may then compete for females on an inter-group level by maximizing the group's peak signal amplitude by synchrony.

Female discrimination toward leading calls may have evolved due to various direct or indirect selection mechanisms[24]. The origin of the preference notwithstanding, males should compete to lead[25,26], particularly if their signals are somehow substandard. An evolutionarily stable means of such competition is inhibitory resetting, and a consequence of collective inhibitory resetting is synchrony. We do not claim that sequence discrimination and intermale signal jamming by inhibitory resetting underlie all synchronous phenomena. But we do establish empirically and theoretically that synchrony can be an incidental by-product[27] of elementary interactions which did not evolve under selection pressure to generate the collective outcome. □

Received 29 December 1992; accepted 19 May 1993.

1. Alexander, R. D. in *Insects, Science, and Society* (ed. Pimentel, D.) 35–77 (Academic, New York, 1975).
2. Wells, K. D. *Anim. Behav.* **25,** 666–693 (1977).
3. Carlson, A. D. & Copeland, J. *Q. Rev. Biol.* **60,** 415–436 (1985).
4. Morin, J. G. *Fla. Ent.* **69,** 105–121 (1986).
5. Walker, T. J. *Science* **166,** 891–894 (1969).
6. Lloyd, J. E. *Nature* **245,** 268–270 (1973).
7. Otte, D. in *How Animals Communicate* (ed. Sebeok, T. A.) 334–361 (Indiana Univ. Press, 1977).
8. Tuttle, M. D. & Ryan, M. J. *Behavl ecol. Sociobiol.* **11,** 125–131 (1982).
9. Buck, J. & Buck, E. *Am. Nat.* **112,** 471–492 (1978).
10. Walker, T. J. & Greenfield, M. D. *Trans. Am. ent. Soc.* **109,** 357–389 (1983).
11. Greenfield, M. D. *Anim. Behav.* **36,** 684–695 (1988).
12. Greenfield, M. D. in *Biology of the Tettigoniidae* (eds Bailey, W. J. & Rentz, D. C.) 71–97 (Springer, Berlin, 1990).
13. Buck, J. *et al. J. comp. Physiol.* A**144,** 277–286 (1981).
14. Hanson, F. E., Case, J. F., Buck, E. & Buck, J. *Science* **174,** 161–164 (1971).
15. Buck, J., Buck, E., Case, J. F. & Hanson, F. E. *J. comp. Physiol.* A**144,** 287–298 (1981).
16. Sismondo, E. *Science* **249,** 55–58 (1990).
17. Maynard Smith, J. & Price, G. R. *Nature* **246,** 15–18 (1973).
18. Partridge, B. L. & Krebs, J. R. *Anim. Behav.* **26,** 959–960 (1978).
19. Maynard Smith, J. *Evolution and the Theory of Games* (Cambridge Univ. Press, 1982).
20. Burk, T. E. *Fla. Ent.* **65,** 90–104 (1982).
21. Belwood, J. J. & Morris, G. K. *Science* **238,** 64–67 (1987).
22. Lakes-Harlan, R. & Heller, K.-G. *Naturwissenschaften* **79,** 224–226 (1992).
23. Robert, D., Amoroso, J. & Hoy, R. R. *Science* **258,** 1135–1137 (1992).
24. Kirkpatrick, M. & Ryan, M. J. *Nature* **350,** 33–38 (1991).
25. Otte, D. & Loftus-Hills, J. *Ent. News* **90,** 159–165 (1979).
26. Greenfield, M. D. & Shaw, K. C. in *Orthopteran Mating Systems: Sexual Competition in a Diverse Group of Insects* (eds Gwynne, D. T. & Morris, G. K.) 1–27 (Westview, Boulder, 1983).
27. Bailey, W. J. *Acoustic Behaviour of Arthropods* (Chapman & Hall, London, 1990).

ACKNOWLEDGEMENTS. We thank the government of Panama for permission to conduct this study, the Smithsonian Tropical Research Institute and especially A. S. Rand for logistical help, R. Ibáñez and F. Solís for field assistance and W. Bailey, W. Bell, R. Gomulkiewicz, K.-G. Heller, B. Ronacher, T. Shelly, O. Stiedl and V. Terwilliger for comments on the manuscript. The work was supported by the NSF and the University of California, Los Angeles.

A possible neuronal basis for representation of acoustic scenes in auditory cortex of the big brown bat

Steven P. Dear, James A. Simmons & Jonathan Fritz

Departments of Neuroscience and Psychology, Box 1853, Brown University, Providence, Rhode Island 02912, USA

BEHAVIOURAL studies[1–4] and field observations[5–7] demonstrate that echolocating bats simultaneously perceive range, direction and shape of multiple objects in the environment as acoustic images derived from echoes. Cortical echo delay-tuned neurons contribute to the perception of object range, because focal inactivation of these neurons disrupts behavioural discrimination of range[8]. We report here that response properties of delay-tuned neurons in the cortical tonotopic area of the bat, *Eptesicus*, transform the sequential arrival times of echoes with different delays into a concurrent, accumulating neural representation of multiple objects at different ranges. The sharpness of delay tuning systematically increases at each best delay in a subpopulation of these neurons while responses to echoes at different delays are accumulated. The resulting concurrent, multiresolution representation of echo delay corresponds to neural implementation of a common representation of images used in computational vision[9–11] and may provide the basis for representing acoustic images of multiple objects as acoustic 'scenes'.

Determination of the distance to objects from echo delay is an important aspect of echolocation in bats[1–3]. In the bat's auditory system, echo delay-tuned neurons encode target range by responding to reception of echoes arriving during a specific time-interval following biosonar vocalizations[12–18]. But echoes returning from multiple objects at different ranges arrive at the bat's ears sequentially, with echoes from nearer objects arriving first. Consequently, neurons tuned to different echo delays receive their stimulation sequentially. How does the bat assemble responses to temporally dispersed echoes from multiple objects at different ranges into a coherent neural representation of an acoustic scene comprising all the objects? Electrophysiological single-unit and multi-unit recordings were made in the auditory cortex of awake big brown bats (*Eptesicus fuscus*) to synthesized pairs of vocalizations and echoes[19]. The tuning and temporal response properties of delay-tuned neurons were characterized. A neuron's delay tuning-curve is a response property defined by the probability of neural discharging for different values of echo delay. Different cortical neurons exhibit different 'best' echo delays (BDs) and different range acuities ($Q_{50\%BD}$) as determined from such curves (Fig. 1*a*). Neurons were tuned to BDs from 2 ms to 28 ms, corresponding to target ranges from 30 to 500 cm, which is the span of biologically relevant ranges for this species[20]. These neurons responded phasically, with an average of just one discharge per emission-echo pair (Fig. 1*b*). The response time for each neuron was measured from the onset of the synthesized vocalization to the neural discharge (vocalization latency, Fig. 1*b*).

A basic requirement for the representation of scenes is a simultaneous or concurrent representation of multiple objects such as an image[21]. The systematic interaction between vocalization latency and BD for neurons from the tonotopic area fulfils this basic requirement by integrating temporally dispersed echoes arriving at the bat's ears from objects at different ranges into a concurrent, cumulative sequence of neural images of range (Fig. 2*a*, *b*). At any instant of time after a vocalization, phasic dis-

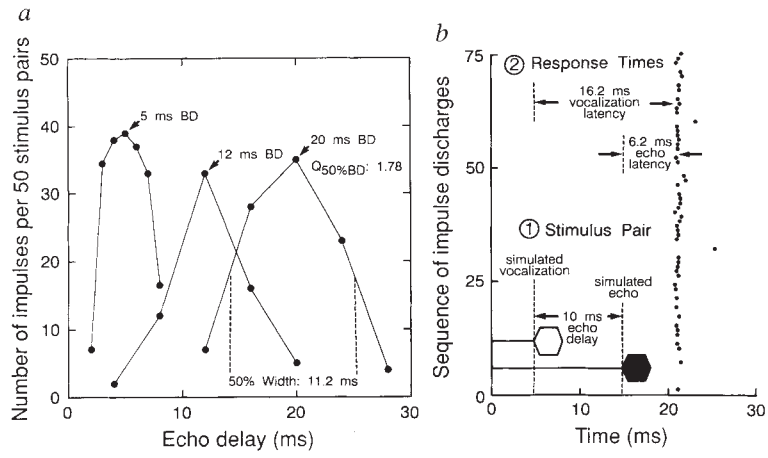

FIG. 1 *a*, Typical delay-tuning curves from three cortical delay-tuned neurons in *Eptesicus*. The optimal stimulus causing the maximal response for each neuron (arrows) is termed best echo delay (BD). These neurons exhibited BDs of 5, 12 and 20 ms, respectively. Delay-tuned neurons also respond to non-optimal values of echo delay. A quality factor, the $Q_{50\%BD}$, is a measure of the sharpness of delay-tuning or range acuity for each neuron, quantified by dividing the BD by the width of the delay-tuning curve at half the maximum response (50% width). The neuron with a 20 ms BD exhibited a 50% width of 11.2 ms, yielding a $Q_{50\%BD}$ of 1.78. *b*, Impulse discharge (dots) of a typical delay-tuned neuron in *Eptesicus* in response to a sound pair (simulated vocalization and echo) with a 10-ms BD. The ensemble of single-unit neurons ($N=33$) responded phasically with an average of 1.1 ± 0.6 action potentials for the combination of a simulated vocalization and an echo at BD. Cortical vocalization latencies ranged from 9.1 to 42.4 ms, with a mean of 25.0 ± 7.2 ms, and echo latencies ranged from 5.6 to 34.4 ms with a mean of 12.1 ± 5.5 ms.

METHODS. Acoustic stimuli were presented free-field directly in front of the bat with a high-frequency leaf tweeter and consisted of pairs of FM sweeps designed to mimic the bat's biosonar vocalization and echo (two harmonics decreasing hyperbolically in frequency, 100 to 50 kHz, 50 to 25 kHz, a duration of 2 ms and a repetition-rate of 5 s^{-1}). Delay-tuning curves were constructed using total impulse counts from peri-stimulus time histograms (PSTHs) in response to either simulated vocalizations, simulated vocalization-echo pairs or single echoes.

charges in the momentarily active ensemble of neurons simultaneously represent the ranges of different objects, collectively forming a neural image of objects at different ranges. The maximum range represented in these neural images is limited by propagation of the bat's biosonar vocalization outward in the environment (Fig. 2*b*). A moment later, a different ensemble of neurons is activated, forming a new neural image of range. This new neural image concurrently represents the ranges of the same objects as before, plus the ranges of objects located at progressively greater distances (Fig. 2*c*). Thus, as time following vocalization elapses and echoes continue to return from objects located incrementally farther away, the discharges of different ensembles of neurons from the tonotopic area form a sequence of neural images representing the ranges of multiple objects. Each neural image concurrently represents multiple objects at different ranges, and successive neural images accumulate new objects out to progressively greater ranges.

Another important requirement for the neural representation of acoustic scenes is the resolution of multiple objects at different ranges. Resolution of range in each successive neural image is related to the relative sharpness of delay-tuning or range acuity of each ensemble of delay-tuned neurons from the tonotopic area. A subpopulation of neurons (sloping solid line, Fig. 3*a*) have two additional response properties specifically related to the resolution of multiple objects at different ranges. First, neurons in each ensemble share the same range acuity (Fig. 3*b*).

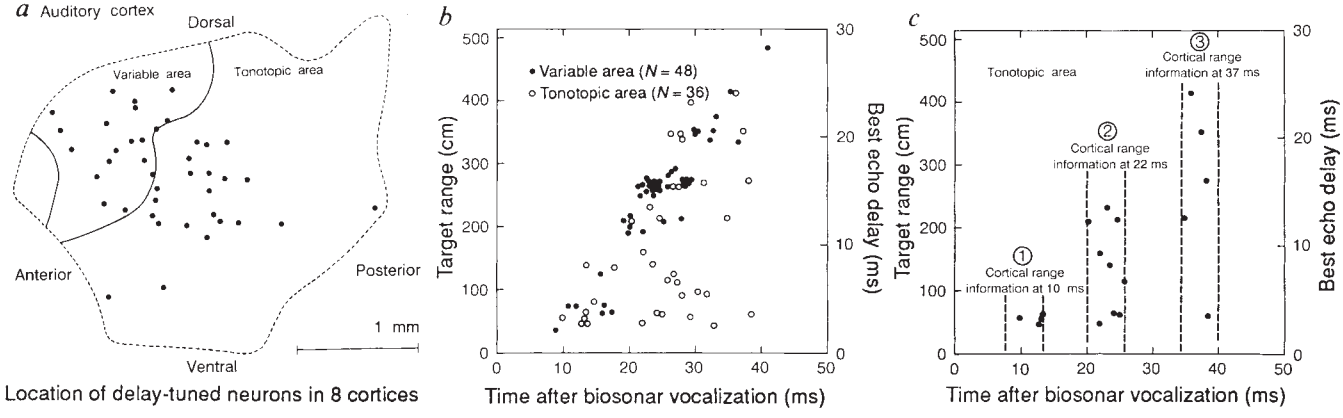

FIG. 2 *a*, A composite of electrode penetrations (dots) containing delay-tuned neurons from the auditory cortex of 8 bats. The dashed line indicates the border of the auditory cortex. We sketched the electrode penetration locations for each bat with the aid of an ocular micrometer in an operating microscope. *b*, Vocalization latencies and BDs of cortical delay-tuned neurons ($N=84$) from the variable (dots) and tonotopic (circles) areas[19]. Vocalization latency is proportional to BD for variable area delay-tuned neurons. Thus, neural responses occur transiently to reflect the sequential arrival of echoes at the bat's ears. In the tonotopic area, many neurons tuned to short ranges have long vocalization latencies. This retards the representation of their short-range estimates until other neurons tuned to longer ranges but with shorter latencies can discharge. As a result, at any instant in time after a vocalization, the phasic discharges of neurons concurrently represent the range of all objects encountered up to the distance set at that moment by the propagation of the bat's biosonar vocalization outward in the environment. This concurrent, cumulative representation is further illustrated in *c* using three subsets of neurons from *b*. At about 10 ms after vocalization in zone 1, neurons discharge to encode ranges of 50 to 85 cm, representing objects relatively near the bat. About 22 ms after vocalization, in zone 2, different neurons discharge to encode ranges around 260 cm. Those neurons that responded immediately to nearer objects in zone 1 are now inactive, but other neurons in zone 2 with short best delays and longer response latencies discharge simultaneously with the longer best-delay neurons to encode ranges from 50 to 260 cm. This systematic trend is continued in zone 3, with neurons simultaneously encoding ranges from 50 cm all the way out to 430 cm.

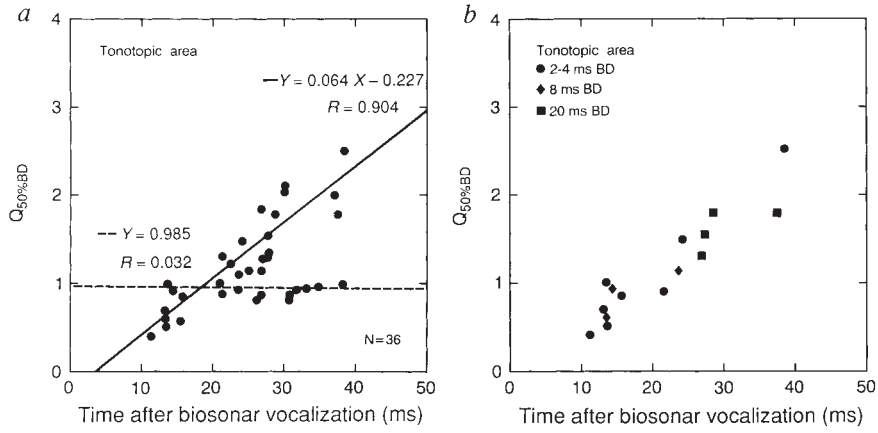

FIG. 3 *a*, A scatterplot of the $Q_{50\%BD}$ or range acuity of delay-tuned neurons from the tonotopic area (dots, $N=36$) against time after the biosonar vocalization. We define a quality factor for expressing the sharpness of tuning or range acuity for each neuron as the $Q_{50\%BD}$, the BD divided by the 50% width (Fig. 1*a*). The visual clustering of neurons suggests a segregation into two subpopulations. The horizontal dashed line represents a linear regression fit to the smaller subpopulation ($N=17$). $Q_{50\%BD}$ represented by the regression is nearly constant, suggesting a constant range acuity for neurons in this subpopulation. The sloping solid line represents a linear regression fit to the larger subpopulation ($N=25$). $Q_{50\%BD}$ is highly correlated with vocalization latency ($R=0.904$), suggesting that the range acuity of neurons in this subpopulation increases proportionally with time after the biosonar vocalization. *b*, Neurons belonging to the subpopulation with increasing range acuity with BDs of 2–4 (dots), 8 (diamonds) or 20 ms (squares). The $Q_{50\%BD}$s of neurons with BDs from 2 to 4 ms systematically increased by a factor of 6.2 with increasing time after the biosonar vocalization. Also, the $Q_{50\%BD}$s of neurons with BDs of 8 ms systematically increased, but only by a factor of 1.9. The $Q_{50\%BD}$s of neurons with BDs of 20 ms systematically increased, but only by a factor of 1.3. Thus, the range of an object is represented with increasing acuity by this subpopulation as the sequence of delay-tuned responses unfolds over the interval following vocalization. The greatest improvement in acuity ultimately occurs for objects located at short ranges, with less improvement for objects at greater ranges.

Second, range acuity systematically improves in sequential ensembles discharging at successively later moments of time after the vocalization (Fig. 3*b*). Consequently, the range of a particular object is represented with increasing acuity by these neurons as the sequence of delay-tuned responses to the same object unfolds in successive neural images (Fig. 4). For each object, the degree of range resolution is proportional to the time following the vocalization in the sequence of neural images (Fig. 4). Taken together, the neural subpopulation provides a multiresolution representation of range, which is important because acoustic scenes contain different-sized objects at different ranges. It is not possible to define a single, optimal range resolution for neural images.

The response properties of the neural subpopulation (Fig. 4) correspond to neural implementation of the well established computational algorithm of multiresolution decomposition[9-11]. A multiresolution decomposition transforms an image or signal into a sequence of images or signals with progressively higher resolutions, providing a common basis for further image or signal processing. For example, multiresolution decompositions are useful in computational vision for edge detection[22,23], object recognition[24-26] and stereo vision[27]. We propose that the concurrent, cumulative, multiresolution representation of target range comprises a computational strategy for echolocation that is specific for the representation of acoustic scenes and distinct from the established principle of computational cortical maps[28].

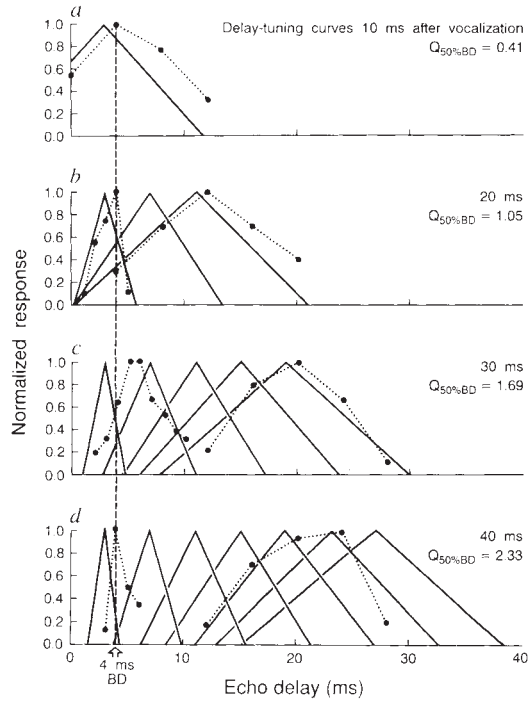

FIG. 4 The relationship between resolution of range and neural images formed by the subpopulation of neurons with increasing range acuity. *a–d*, Actual delay-tuning curves (dotted lines) are superimposed on schematic delay-tuning curves (solid lines). BDs of schematic delay-tuning curves are spaced 4 ms apart for illustrative clarity. All neurons exhibit the same $Q_{50\%BD}$ in each of the four neural images. Consequently, the widths of all delay-tuning curves for neurons in each neural image are proportional to BD. But because $Q_{50\%BD}$ systematically increases with time, all delay-tuning curves are narrower in successive neural images. Thus, for a single object located at a range corresponding to an echo delay of 4 ms (vertical dashed line), the acuity of neurons representing this object's range increases in successive neural images (*a*, *b*, *d*). Although this increase in range acuity seems unnecessary for the representation of single objects, the increase is directly related to resolution of multiple objects at different ranges. Two objects at ranges corresponding to echo delays of 3 to 5 ms cannot be resolved in the neural image at 10 ms after vocalization because both objects cause the same delay-tuned neurons to discharge. By 40 ms after vocalization, the range of each object can now be encoded by separate delay-tuned neurons due to the increased range acuity of the neurons in the later neural image. Thus, closely spaced objects can first be resolved in a neural image at a time after vocalization inversely proportional to the difference in range between the objects. The degree of range resolution in neural images depends on the absolute ranges of the objects. Multiple objects located at progressively greater ranges are represented with progressively less resolution. Less resolution is needed at greater ranges due to range distortions introduced by the flight of the bat.

Our results suggest that a sequence of multiresolution images of range in the tonotopic area of cortex may provide the basis for building a representation of multiple objects as acoustic scenes in *Eptesicus*. □

Received 11 January; accepted 17 June 1993.

1. Griffin, D. R. *Listening in the Dark* (Yale Univ. Press, New Haven, 1958).
2. Simmons, J. A. *Science* **171,** 925 (1971).
3. Simmons, J. A. *J. acoust. Soc. Am.* **54,** 157 (1973).
4. Webster, F. A. & Brazier, O. G. *Clearing House for Federal Scientific and Technical Information*, Springfield, VA Technical Report AMRL-TR-67-192 (1968).
5. Griffin, D., Friend, J. H. & Webster, F. A. *J. exp. Zool.* **158,** 155 (1965).
6. Schnitzler, H.-U. & Henson, O. W. in *Animal Sonar Systems* (eds Busnel, R.-G. & Fish, J. F.) 109–181 (Plenum, New York, 1980).
7. Neuweiler, G. *Physiol. Rev.* **70,** 615 (1990).
8. Riquimaroux, H., Gaioni, S. J. & Suga, N. *Science* **251,** 565 (1991).
9. Witkin, A. P. *IEEE ICASSP Proceedings* **39A.1.1** (1984).
10. Mallat, S. G. *IEEE Trans. Acoust. Speech Signal Processing* **37,** 2019 (1989).
11. Akansu, A. N. & Haddad, R. A. *Multiresolution Signal Decomposition* (Academic, Boston, 1992).
12. Feng, A. S., Simmons, J. A. & Kick, S. A. *Science* **202,** 645 (1978).
13. Suga, N., O'Neill, W. E. & Manabe, T. *Science* **200,** 778 (1978).
14. O'Neill, W. E. & Suga, N. *Science* **203,** 69 (1979).
15. Sullivan, W. E. *J. Neurophysiol.* **48,** 1011 (1982).
16. Wong, D. & Shannon, S. L. *Brain Res.* **453,** 349 (1988).
17. Berkowitz, A. & Suga, N. *Hearing Res.* **41,** 255 (1989).
18. Schuller, G., O'Neill, W. E. & Radtke-Schuller, S. *Eur. J. Neurosci.* **3,** 1165 (1991).
19. Dear, S. P., Fritz, J. Haresign, T., Ferragamo, M. & Simmons, J. A. *J. Neurophysiol.* (in the press).
20. Kick, S. A. & Simmons, J. A. *J. Neurosci.* **4,** 2725 (1984).
21. Marr, D. *Vision* (Freeman, San Francisco, 1982).
22. Rosenfeld, A. & Thurston, M. *IEEE Trans. Computers* C**20,** 562 (1971).
23. Marr, D. & Hildreth, E. C. *Proc. R. Soc.* B**207,** 187 (1980).
24. Burt, P. J., Hong, T. H. & Rosenfeld, A. *IEEE Trans. Syst. Man. Cybern.* **11,** 802 (1981).
25. Hong, T. H. & Shneier, M. *IEEE Trans. Pattern Analyt. Machine Intel.* **6,** 229 (1984).
26. Hong, T. H. & Rosenfeld, A. *IEEE Trans. Pattern Analyt. Machine Intel.* **6,** 222 (1984).
27. Marr, D. & Poggio, T. *Proc. R. Soc.* B**204,** 301 (1979).
28. Suga, N. *Neural Networks* **3,** 3 (1990).

ACKNOWLEDGEMENTS. We thank T. Haresign for writing the computer software used for generating our acoustic stimuli, T. Haresign, C. F. Moss and M. Ferragamo for experimental work, and A. Simmons, B. Connors and J. McIlwain for comments on the manuscript. This research was supported by grants from ONR, NIMH and NSF.

Postsynaptic control of plasticity in developing somatosensory cortex

Bradley L. Schlaggar*, Kevin Fox† & Dennis D. M. O'Leary*‡

* Molecular Neurobiology Laboratory, 10010 N. Torrey Pines Road, Salk Institute, La Jolla, California 92037, USA
† Department of Physiology, University of Minnesota, Minneapolis, Minnesota 55455, USA

THE rearrangement of synaptic connections during normal and deprived development is thought to be controlled by correlations in afferent impulse activity[1]. A favoured model is based on postsynaptic detection of synchronously active afferents; synapses are stabilized when pre- and postsynaptic activity is correlated and weakened or eliminated when their activity is uncorrelated[2,3]. Most evidence for this model comes from demonstrations that correlated afferent input is necessary for the segregation of eye-dominant inputs in the developing vertebrate visual system[1,4,5] and that critical period plasticity of ocular dominance columns in cat visual cortex is disrupted by blockade of postsynaptic transmission[6–8]. We tested whether the developmental plasticity of somatosensory columns, known as 'barrels', in rodent primary somatosensory cortex (S1)[9–13] is similar to that of ocular dominance columns. We report here that the selective disruption of postsynaptic activation in rat S1 by application of a glutamate receptor antagonist inhibits rearrangements in the somatotopic patterning of thalamocortical afferents induced by manipulations of the sensory periphery during the critical period. These findings show that postsynaptic activation has a prominent role in critical period plasticity in S1 cortex.

Barrels of S1 cortex are composed of discrete aggregates of layer 4 neurons[9] innervated by clusters of ventroposterior thalamocortical (VP) afferents[11] arranged in a somatotopic pattern isomorphic to that of the large sensory vibrissae on the rodent's muzzle[9,11]. VP afferents are diffusely distributed in S1 of newborn

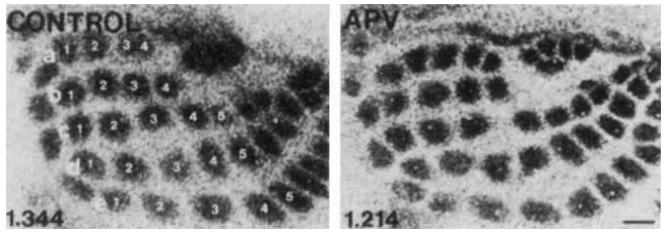

FIG. 1 Chronic postnatal APV treatment does not disrupt the emergence of a normal barrel pattern in rat S1 cortex. Bright-field photomicrographs of sections through rat S1 cut tangential to the pial surface and reacted for acetylcholinesterase, a marker of the distribution of ventroposterior thalamocortical afferents to S1. In control-Elvax-treated hemispheres (Control), the degree of patterning here does not differ from normal barrel patterning in unoperated rats (not shown). Afferent patches corresponding to the barrels measured for row and barrel field area are labelled by convention. APV treatment (APV) does not appear to interfere with the emergence of patterning of thalamocortical afferents when assayed with AChE histochemistry. Numbers in bottom corner are D/C ratio value for particular hemisphere. In normal, noncauterized animals, the D/C ratio values did not differ between normal pups (1.259 ± 0.051; mean ± s.e.m.; $n = 10$) and control-Elvax treated pups (1.2281 ± 0.026; $n = 18$). The latter were indistinguishable from APV-Elvax treated pups (1.264 ± 0.041; $n = 10$).
METHODS. Sprague–Dawley rats ranging in age from P0 to P8 (P0 refers to the first 24 h after birth), obtained from timed pregnant females (Harlan–Sprague–Dawley, Omaha), were used for this study. In all litters, the time of birth was noted. Elvax (Dupont) with either 10 mM D-APV (the active isomer) or 0.1 mM L-APV (the inactive isomer; G. Prusky and M. Constantine-Paton) was prepared as described previously[25]. Elvax was implanted subdurally over the right S1 in hypothermic P0 animals at ~6 h postnatal. In each pup a triangular piece (width 2 mm, length 3 mm, thickness 90 μm) of APV-Elvax (with D-APV) or control-Elvax (with L-APV) was inserted subdurally over S1. Pups were returned to their mother after recovery. At P8, pups were killed with pentobarbital and perfused with 0.9% saline than 10% formalin in 0.1 M phosphate buffer (pH 7.4). Cerebral cortices were removed, flattened, post-fixed overnight and cryoprotected (25% sucrose, 10% formalin in 0.1 M phosphate buffer). Cortices were sectioned (50 μm on a freezing microtome), washed (0.1 M phosphate buffer), mounted (every section from pia to white matter) on gelatin-coated slides, air dried, and processed with the indirect AChE histochemical method[29]. AChE is transiently expressed on the axons of VP thalamic projection neurons and intensely marks their cortical terminations which innervate the barrels, thereby revealing the barrel pattern[15,17]. The AChE-dense, patterned terminations of VP thalamocortical afferents are distinct from a diffuse low level background of AChE staining of a proportion of cortical cells. Data analysis: to quantify the effect of APV on the development of barrel cortex and its plasticity after C row cautery, we devised a simple measurement scheme referred to as the D/C ratio. The surface area devoted to each barrel row was measured using Sigmascan software (Jandel) from projection lamp drawings of each analysed hemisphere. The barrels included in the row measurement are shown in the figure. For every hemisphere, the area of each row was normalized for total barrel-field size and expressed as a percentage. Next, the D/C ratio was calculated by dividing D row normalized area by that of C row. Thus, the D/C ratio gives a single numerical value to the relative territory devoted to rows D and C and the relative areal increase of D row and decrease of C row in a single hemisphere following peripheral lesion. This standardization corrects for cortical flattening artefacts, normalizes for overall barrel-field size, provides an index for plasticity in both a deprived and nondeprived row, and aids in measuring the degree of variation of plasticity following vibrissae follicle row cautery.

‡ To whom correspondence should be addressed.